Electronic structure of the misfit layer compound $(SnS)_{1.20}TiS_2$: band structure calculations and photoelectron spectra

1996 J. Phys.: Condens. Matter 8 1663

(http://iopscience.iop.org/0953-8984/8/11/011)

J. Phys.: Condens. Matter **8** (1996) 1663–1676. Printed in the UK

Electronic structure of the misfit layer compound $(SnS)_{1.20}TiS_2$: band structure calculations and photoelectron spectra

C M Fang, R A de Groot, G A Wiegers and C Haas

Chemical Physics, Materials Science Centre of the University, Nijenborgh 4, 9747 AG Groningen, The Netherlands

Received 25 October 1995

Abstract. In order to understand the electronic structure of the incommensurate misfit layer compound $(SnS)_{1.20}TiS_2$ we carried out an *ab initio* band structure calculation in the supercell approximation. The band structure is compared with that of the components 1T-TiS_2 and hypothetical SnS with a similar structure as in $(SnS)_{1.20}TiS_2$. The calculations show that the electronic structure is approximately a superposition of the electronic structures of the two components TiS_2 and SnS, with a small charge transfer from the SnS layer to the TiS_2 layer. The interlayer bonding between SnS and TiS_2 is dominated by covalent interactions. X-ray and ultraviolet photoelectron spectra of the valence bands are in good agreement with the band structure calculation.

1. Introduction

An interesting class of materials called 'misfit layer compounds' is characterized by the general formula $(MX)_{1+x}TX_2$ (M = Sn, Pb, Bi, Sb, or rare earth metal; X = S, Se; T = Ti, V, Cr, Nb, Ta; and $0.08 < x < 0.26$) and planar intergrowth structures [1–4]. The structure consists of alternating MX double layers and TX_2 sandwiches, which do not match; these compounds lack therefore three-dimensional periodicity. The misfit layer compounds are very stable: the crystals are grown at high temperatures (700–1200 °C) and prefer regular over random stacking of the layers. For a better understanding of the stability and the chemical bonding between the two subsystems MX and TX_2 the knowledge of the electronic band structure is important.

$(SnS)_{1.20}TiS_2$ is built of alternating SnS double layers with distorted rocksalt-type structure and TiS_2 sandwiches slightly distorted compared with 1T-TiS_2; both subsystems are triclinic [5]. $(SnS)_{1.20}TiS_2$ has n-type metallic electrical conduction, with an electron concentration of about 0.2 electrons/Ti as was deduced from Hall effect measurements [6]. Resistivity measurements showed a strong anisotropy with a ρ_c/ρ_{ab} ratio of about 10^2–10^3 [1, 6]. On the basis of x-ray photoemission (XPS), x-ray absorption (XAS), and electron energy loss (EELS) studies, Ohno concluded that the valence band structure is well represented by a simple superposition of the electronic structure of each layer, except for charge transfer from the SnS to the TiS_2 layers [7]. From XPS Ettema and Haas concluded that the interlayer charge transfer is absent or small, and that the stability is due to covalent interlayer bonding [8]. From Raman scattering of the misfit compounds $(SnS)_{1.20}NbS_2$, $(PbS)_{1.14}NbS_2$, and $(PbS)_{1.18}TiS_2$ Hangyo and co-workers found that the

0953-8984/96/111663+14$19.50

spectra are a superposition of the intralayer vibrations of individual layers, which indicates a weak interlayer interaction. The shift of the intralayer Raman modes of TS_2 in the misfit compounds relative to those of 1T-TiS_2 (or 2H-NbS_2) was interpreted in terms of a charge transfer from the MS layer to the TS_2 layer [9, 10].

So far only the electronic structure of the related commensurate compound $(SnS)_{1.20}NbS_2$, in which the SnS subsystem had to be compressed by about 2.5%, has been calculated [11]. In this work we present a study of the electronic structure of the misfit compound $(SnS)_{1.20}TiS_2$ using *ab initio* band structure calculations and photoelectron spectra.

Table 1. Unit cell dimensions, space group (S.G.) and number Z of formula units of the subsystems of $(SnS)_{1.20}TiS_2$.

	a (Å)	b (Å)	c (Å)	α (°)	β	γ	S.G.	Z
SnS	5.683	5.834	11.680	95.83	94.78	90.03	$C\bar{1}$	4
TiS_2	3.412	5.834	23.289	95.86	90.30	90.01	$F\bar{1}$	4

Table 2. Fractional coordinates of $(SnS)_{1.17}TiS_2$ for the atoms in the subsystems SnS and TiS_2, expressed in terms of the unit cells of the subsystems of table 1. WP is the Wyckoff position.

SnS	WP	x	y	z	TiS_2	WP	x	y	z
Sn	4(a)	−0.0225	−0.2806	0.3700	Ti	2(a)	1/4	1/4	0
S(1)	4(a)	0.160	−0.2320	0.5954	S(2)	4(a)	0.2480	0.5587	−0.061 75

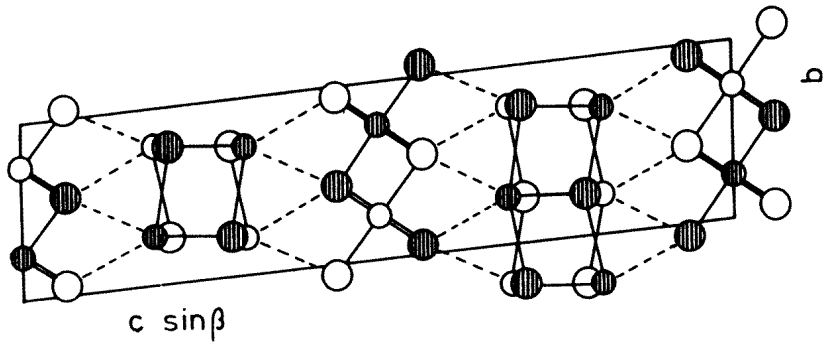

Figure 1. The crystal structure of $(SnS)_{1.20}TiS_2$ projected along [100]. Small circles are Ti (at the bottom, middle, and top) and Sn, large circles are S atoms. Atoms of the same subsystem $a/2$ apart are indicated by open and filled circles of the same size. Broken lines indicate the interaction of Sn with S of the TiS_2 layer.

2. Structure of $(SnS)_{1.20}TiS_2$

The two subsystems, SnS and TiS_2, of $(SnS)_{1.20}TiS_2$ are triclinic with unit cells given in table 1 [5]. The in-plane vectors are $\boldsymbol{a}$ and $\boldsymbol{b}$. The $\boldsymbol{b}$ vectors are parallel and of equal length

while the $\boldsymbol{a}$ vectors, being parallel, have different lengths (note the subsystems 1 and 2 refer to the SnS and the TiS_2 subsystem, respectively). The space groups are $C\bar{1}$ for SnS and $F\bar{1}$ for TiS_2. These centred space groups are chosen in order to facilitate comparison with other misfit layer structures. The c axis of TiS_2 (c_2) is approximately twice that of SnS (c_1) because of the different centring. This approximation is used because the two axes diverge ($\beta_1 \neq \beta_2$). Coordinates of the atoms are given in table 2. The SnS part of the structure consists of deformed slices of SnS with a thickness of half the cell edge of the (hypothetical) distorted NaCl-type SnS. Each Sn atom is coordinated by five S atoms within the same double layer and at larger distances by two or three S atoms of the TiS_2 layers. The SnS double layer is corrugated with the Sn atoms on the outside (figure 1). The Sn bond distance to the apex S atom of the SnS double layer, in projection almost parallel to the $\boldsymbol{c}$ axis, is much shorter (2.610(3) Å) than the other four Sn–S distances which are 2.866(4), 2.873(4), 2.911(4), and 2.976(1) Å. The same phenomenon is observed for the SnS double layer in $(SnS)_{1.17}NbS_2$. The TiS_2 sandwich is slightly distorted compared to 1T-TiS_2. The Ti–S distances and S–Ti–S angles show that the symmetry of a TiS_6 polyhedron is close to $2/m$ (note that the space group of 1T-TiS_2 in the $a \times a\sqrt{3}$ orthohexagonal cell is $C2/m$). The Ti–S distances (average 2.45 Å) are close to those observed in 1T-TiS_2, 2.4297 Å. The two subsystems mutually modulate each other incommensurately, which means that the structure described by the three-dimensional space groups of the two subsystems is only the average structure. The complete structure, including the mutual modulation, is described by a $(3+1)$-dimensional superspace group [3, 5].

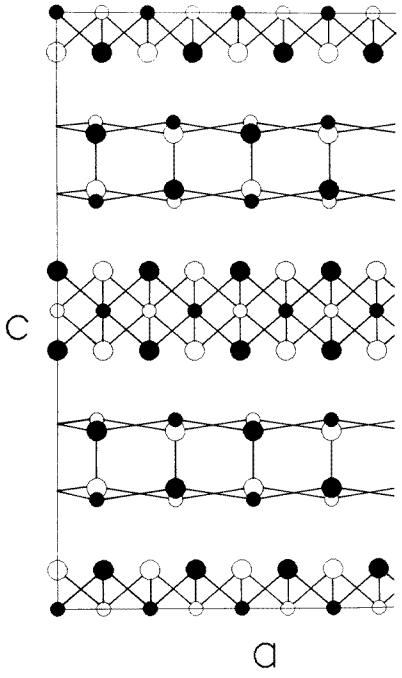

Figure 2. A projection of the structure of $(SnS)_{1.20}TiS_2$ along [010] in the commensurate approximation with $\beta_1 = \beta_2 = 90°$. The origin is chosen at Ti.

Since the existing computer programs for band structure calculations cannot be used to calculate the electronic structure of modulated crystals, the simplest way to perform

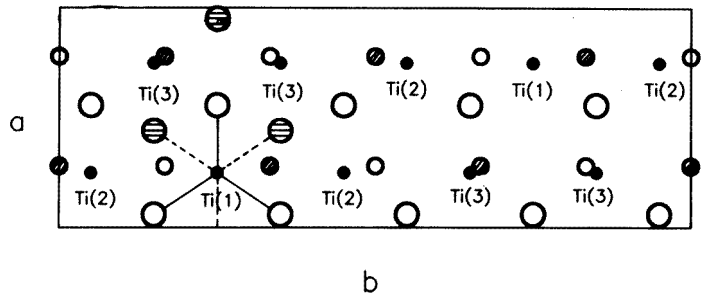

Figure 3. A projection of half of the unit cell of $(SnS)_{1.20}TiS_2$ along [001] in the large supercell, space group $C2/c$. Along a five unit cells of TiS_2 correspond with three unit cells of SnS. Large open circles are S atoms of the TiS_2 subsystem. S atoms of the SnS subsystem are not indicated for sake of clarity. Small open (dashed) and filled circles are Sn and Ti, respectively. For one Ti the full octahedral coordination by S is indicated.

a calculation of the band structure is to make the incommensurate crystal structure commensurate. For $(SnS)_{1.20}TiS_2$ the simplest commensurate approximation consists of five units TiS_2 and three units SnS along [100] while the diverging $\boldsymbol{c}$ axes have to be brought to a common $\boldsymbol{c}$ axis (figure 2). By taking $\beta_1 = \beta_2 = 90^\circ$ and $c \approx 2c_1 \approx c_2$ one obtains a supercell with $a = 17.065$ Å ($= 5a_{TiS_2} \approx 3a_{SnS}$), $b = 5.834$ Å, $c = 23.29$ Å, $\alpha = 95.85^\circ$, $\beta = \gamma = 90^\circ$. The a axis was chosen equal to five times a_{TiS_2} since the TiS_2 part is the more rigid one of the two subsystems. The SnS part is almost the same as in the misfit layer structure with the a axis enlarged by less than 0.1%. In this supercell, the origin along [100] of one lattice with respect to the other can be chosen arbitrarily; an arbitrary choice leads to a C-centred lattice with 12 Sn, 10 Ti, and 32 S as crystallographically independent atoms (cell content $(SnS)_{24}(TiS_2)_{20}$). By choosing the origin of SnS with respect to TiS_2 as shown in figure 3, the arrangment is described by the monoclinic space group $C2/c$ with cell parameters $a = 5.834$ Å, $b = 17.065$ Å, $c = 23.29$ Å, and $\beta = 95.85^\circ$ (note that these axes are chosen according to the setting in the International Tables). All atoms are on general sites 8(f), except Ti(1) which is on site 4(d). The crystallographically independent atoms are therefore reduced to three Ti, three Sn, and eight S atoms. The coordinates are such that the intralayer distances between atoms of the SnS and TiS_2 layers are the same as in the misfit layer structure.

3. Bond length and bond strength

The bond distances of the misfit layer compound $(SnS)_{1.20}TiS_2$ are listed in table 3. Some insight into the bonding can be obtained by using the concept of bond valence [12]. The bond valence V_i is calculated from the relation $V_i = \exp[(d_0 - d_i)/b]$, where d_i is the distance between the atoms of bond i, and d_0 and b are empirical constants: $d_0 = 2.45$ Å for Sn–S and $b = 0.37$ Å [13]. The bond valence or oxidation state V of an atom is calculated by summing over all neighbouring atoms $V = \sum V_i$. For comparison the Sn–S distances and bond valences of α- and β-SnS are included in table 3.

The sum $\sum V_i$ of the contributions of intralayer Sn–S bonds to the valence of Sn is somewhat smaller for $(SnS)_{1.20}TiS_2$ (1.81) than for α-SnS (2.02) and for β-SnS (1.88). In α- and β-SnS there is very weak interlayer bonding, with $V = 0.079$ for α-SnS (one interlayer Sn–S bond of 3.388 Å) and $V = 0.072$ for β-SnS (two interlayer Sn–S bonds of 3.74 Å).

Table 3. Interatomic distances d_i (Å) and bond valences V_i in the misfit layer compound $(SnS)_{1.20}TiS_2$ compared with α- and β-SnS.

Bonds in the SnS layers					
d_i (Å)	V_i				
1×2.866	0.325				
1×2.873	0.319				
1×2.933	0.271				
1×2.976	0.241				
1×2.610	0.649				
$V = \sum V_i$	1.805				
Bonds between Sn in the SnS layer and S in the TiS_2 layer					
Sn(1)		Sn(2)		Sn(3)	
d_i	V_i	d_i	V_i	d_i	V_i
1×3.494	0.06	1×3.385	0.08	1×3.085	0.18
1×3.187	0.14	1×3.399	0.08		
$V = \sum V_i$	0.20		0.16		0.18
Sn–S bonds in α- and β-SnS					
α-SnS		β-SnS			
d_i (Å)	V_i	d_i (Å)	V_i		
1×2.627	0.620	1×2.59	0.685		
2×2.665	0.559	4×2.96	0.281		
2×3.290	0.103	2×3.74	0.036		
1×3.388	0.079				
$V = \sum V_i$	2.02		1.88		

The interlayer bonding in the misfit layer compounds is much stronger. For $(SnS)_{1.20}TiS_2$ the contribution of interlayer bonds to the Sn valence is 0.20, 0.16, and 0.18 for Sn(1), Sn(2), and Sn(3), respectively. In the incommensurate structure the interlayer Sn–S bond valence shows a continuous range of values; the average value is 0.20.

The total valence of Sn in $(SnS)_{1.20}TiS_2$, obtained by adding the contributions of interlayer and intralayer bonds, is about two, close to the values in α- and β-SnS.

4. Band structure calculations

4.1. Method of the calculations

Ab initio band structure calculations were performed with the lcoalized spherical wave (LSW) method [15] using a scalar-relativistic Hamiltonian. The LSW method is a modified version of the augmented spherical wave (ASW) method [16]. We used local-density exchange–correlation potentials [17] inside space-filling, and therefore overlapping, spheres around the atomic constituents. The self-consistent calculations were carried out including all core electrons.

Iterations were performed with $\boldsymbol{k}$ points distributed uniformly in an irreducible part of the first Brillouin zone (BZ), corresponding to a volume of the BZ per $\boldsymbol{k}$ point of the order of 1.5×10^{-5} Å^{-3}. Self-consistency was assumed when the changes in the lcoal partial charges in each atomic sphere decreased to the order of 10^{-5}.

In the construction of the LSW basis [15, 18], the spherical waves were augmented by solutions of the scalar-relativistic radial equations indicated by the atomic-like symbols, 5s, 5p, 5d; 4s, 4p, 3d; and 3s, 3p, 3d corresponding to the valence levels of the parent elements Sn, Ti, and S, respectively. The internal l summation, used to augment a Hankel function at surrounding atoms, was extended to $l = 3$, resulting in the use of 4f orbitals for Sn and Ti. When the crystal is not very densely packed, as is the case in layered materials such as $(SnS)_{1.20}TiS_2$, SnS, and TiS_2, it is necessary to include empty spheres in the calculations. The functions 1s and 2p, and 3d as an extension, were used for the empty spheres. The input parameters (lattice constants, Wigner–Seitz sphere radii) are listed in table 4.

Table 4. Input parameters for the band structure calculation of $(SnS)_{1.20}TiS_2$. WP is the Wyckoff position. The empty spheres are indicated by Va, and the radii of the muffin-tin spheres of Sn, Ti, and S by R_{WS} (Å).

Supercell space group $C2/c$ (No 15)
$a = 5.834$ Å
$b = 17.065$ Å
$c = 23.29$ Å
$\beta = 95.85^\circ$
$V = 2306.6$ Å^3, cell content $(SnS)_{24}(TiS_2)_{20}$

Atoms	WP	Coordinates	R_{WS} Å
Ti(1)	4c	(0.2500, 0.2500, 0.000)	1.1916
Ti(2)	8f	(0.2500, 0.0500, 0.000)	1.1916
Ti(3)	8f	(0.2500, 0.6500, 0.000)	1.1916
S(1)	8f	(0.5587, 0.0500, −0.061 75)	1.8305
S(2)	8f	(0.5587, 0.2500, −0.061 75)	1.8305
S(3)	8f	(0.5587, 0.4500, −0.061 75)	1.8305
S(4)	8f	(0.5587, 0.6500, −0.061 75)	1.8305
S(5)	8f	(0.5587, 0.8500, −0.061 75)	1.8305
Sn(1)	8f	(0.7394, 0.0000, 0.1850)	1.2444
Sn(2)	8f	(0.7194, 0.3333, 0.1850)	1.2444
Sn(3)	8f	(0.7194, 0.6667, 0.1850)	1.2444
S(6)	8f	(0.7680, 0.0000, 0.2977)	2.0167
S(7)	8f	(0.7680, 0.3333, 0.2977)	2.0167
S(8)	8f	(0.7680, 0.6667, 0.2977)	2.0167
Va(1)	8f	(0.2587, 0.0820, 0.1230)	0.8889
Va(2)	8f	(0.1880, 0.7750, 0.1235)	0.8889
Va(3)	4e	(0.0000, 0.0833, 0.2500)	0.8889
Va(4)	4e	(0.0000, 0.9167, 0.2500)	0.8889
Va(5)	4e	(0.0000, 0.2500, 0.2500)	0.8889
Va(6)	4e	(0.0000, 0.7500, 0.2500)	0.8619
Va(7)	4e	(0.0000, 0.4166, 0.2500)	0.9158
Va(8)	4e	(0.0000, 0.5833, 0.2500)	0.9158

4.2. The band structures of the two components TiS_2 and SnS

For a better understanding of the band structure of $(SnS)_{1.20}TiS_2$ it is useful to compare the results of the calculations with band structure of the two components SnS and TiS_2. Detailed calculations were reported for α- and β-SnS [14]. However, the structure of the SnS double layers in α- and β-SnS is quite different from that in the misfit layer compound

$(SnS)_{1.20}TiS_2$. Therefore we have carried out a band structure calculation for a hypothetical SnS crystal, with layers similar to those in the misfit layer structure. The unit cell dimensions are taken as equal to those of the SnS subsystem in $(SnS)_{1.20}TiS_2$ except for the length of the c axis which was chosen such that the interlayer Sn–S distances are 3.4–3.5 Å, similar to those between Sn and S of the TiS_2 layer in the misfit layer compound and those in α-SnS. The space group is $C\bar{1}$. The input parameters for the band structure calculations are given in table 1.

Table 5. Input parameters for band structure calculations of hypothetical SnS.

SnS triclinic, space group $P\bar{1}$ $a = 5.683$ Å, $b = 5.832$ Å, $c = 6.0736$ Å $\alpha = 95.85°$, $\beta = 94.78°$, $\gamma = 90°$					
		Coordinates			
	WP	x	y	z	R_{WS} (Å)
Sn(1)	2i	(0.0225, 0.2806, 0.2500)			1.2678
Sn(2)	2i	(0.4775, 0.2194, 0.7500)			1.2678
S(1)	2i	(0.0160, −0.2320, 0.3165)			1.9758
S(2)	2i	(0.5160, 0.2680, 0.3165)			1.9758
Va(1)	2i	(0.7500, 0.0000, 0.0000)			1.2952
Va(2)	2i	(0.2500, 0.5000, 0.0000)			1.2897

Hypothetical SnS is a semiconductor with a band gap of 1.05 eV; the total and partial densities of states (DOSs) are shown in figure 4. For a detailed discussion of band structure and chemical bonding in SnS we refer to [11] and [14].

Several good band structure calculations are available for 1T-TiS_2 [19–21]. In order to compare with the band structure of the misfit layer compound we have calculated the band structure of 1T-TiS_2 using the LSW method, coordinates were from [22]. The total and partial DOSs are shown in figure 5. The band structure of 1T-TiS_2 is similar to that of previous calculations. In this calculation we find an indirect overlap of about 0.6 eV between top of the S 3p valence band in Γ and the bottom of the Ti 3d conduction band in L.

4.3. Band structure of $(SnS)_{1.20}TiS_2$

The first BZ corresponding to the large unit cell with space group $C2/c$ (No 15) is shown in figure 6. The dispersion of the bands in the region -15.0–-11.0 eV (mainly S 3s) and near the Fermi level is shown in figure 7(a) and (b), respectively, for selected directions in the BZ. The total and partial DOSs obtained from the band structure calculation are shown in figure 8. The charges on the Wigner–Seitz spheres and the orbital configurations of atoms and empty spheres are given in table 6. We remark that not too much significance should be attributed to differences in charge and orbital configuration, as these numbers are strongly dependent on the Wigner–Seitz radii, and the presence of empty spheres. The variation of the electronic configuration of one type of atom within a subsystem is small; this indicates that the modulation of the electronic structure of one subsystem by the other subsystem is small. There is a small, but significant, difference between the electronic configuration of S in TiS_2 and the SnS subsystems, but this is at least partly due to the different Wigner–Seitz radii.

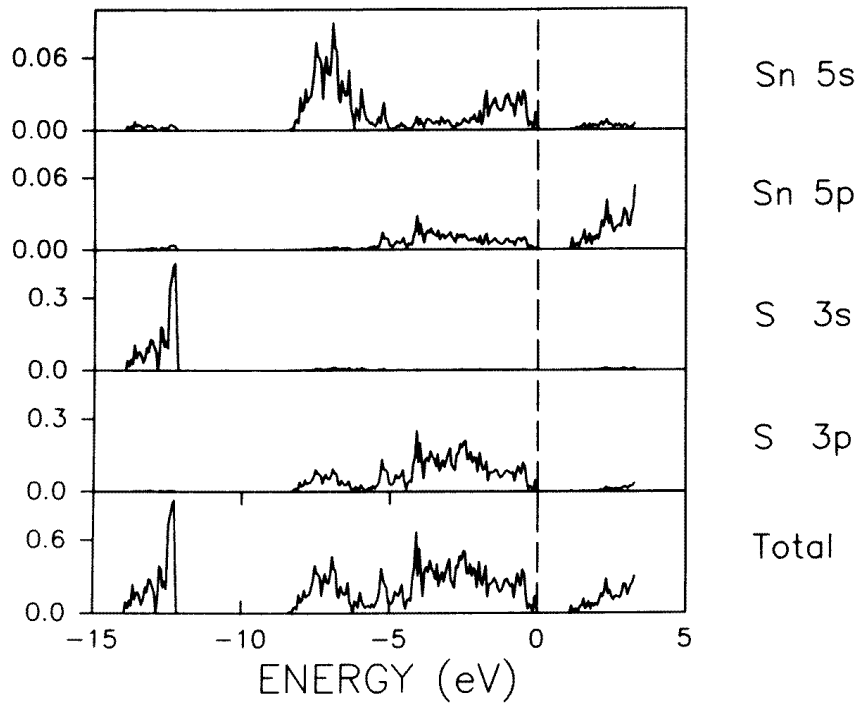

Figure 4. The total and partial DOSs of the hypothetical SnS.

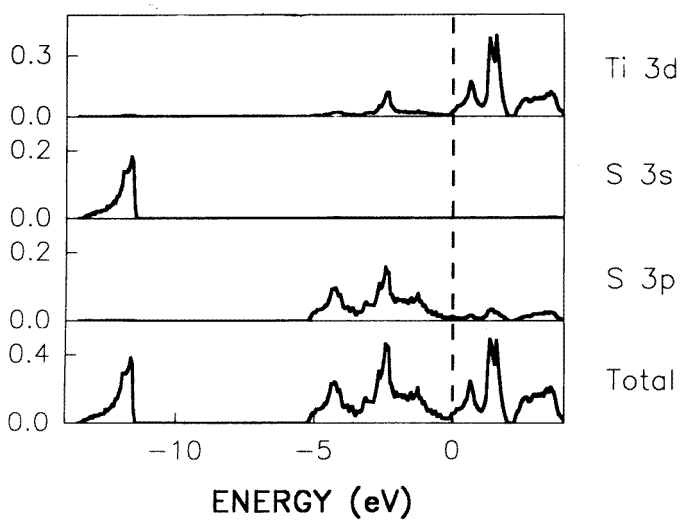

Figure 5. The total and partial DOSs of 1T-TiS_2.

The lowest bands mainly consist of S 3s orbitals, with in the lower part mainly S 3s of the TiS_2 subsystem, whereas the S 3s states of the SnS subsystem are at the top of these bands. There is a shift of about 1.3 eV to lower energy of the top of S 3s band of the TiS_2

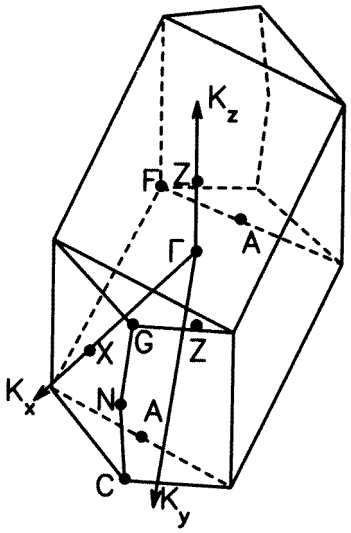

Figure 6. The BZ and high-symmetry points of $(SnS)_{1.20}TiS_2$ with space group $C2/c$.

Table 6. Electronic configurations of the atoms in $(SnS)_{1.20}TiS_2$.

Atom	R_{WS} Å)	Electronic configuration
TiS_2 subsystem		
Ti(1)	1.1916	[Ar] $4s^{0.13}4p^{0.20}3d^{1.67}4f^{0.03}$
Ti(2)	1.1916	[Ar] $4s^{0.13}4p^{0.20}3d^{1.66}4f^{0.03}$
Ti(3)	1.1916	[Ar] $4s^{0.14}4p^{0.20}3d^{1.65}4f^{0.03}$
S(1)	1.8305	[Ne] $3s^{1.93}3p^{5.06}3d^{0.25}$
S(2)	1.8305	[Ne] $3s^{1.93}3p^{5.02}3d^{0.25}$
S(3)	1.8305	[Ne] $3s^{1.96}3p^{5.03}3d^{0.25}$
S(4)	1.8305	[Ne] $3s^{1.94}3p^{5.04}3d^{0.25}$
S(5)	1.8305	[Ne] $3s^{1.94}3p^{5.00}3d^{0.26}$
SnS subsystem		
Sn(1)	1.2444	[[Kr] $4d^{10}$] $5s^{1.18}5p^{0.38}4f^{0.01}$
Sn(2)	1.2444	[[Kr] $4d^{10}$] $5s^{1.16}5p^{0.34}5d^{0.05}4f^{0.01}$
Sn(3)	1.2444	[[Kr] $4d^{10}$] $5s^{1.16}5p^{0.37}5d^{0.05}4f^{0.01}$
S(6)	2.0167	[Ne] $3s^{2.03}3p^{5.20}3d^{0.47}$
S(7)	2.0167	[Ne] $3s^{2.02}3p^{5.23}3d^{0.52}$
S(8)	2.0167	[Ne] $3s^{2.04}3p^{5.24}3d^{0.53}$

subsystem in the misfit layer compound with respect to the bottom of the Ti $4d_{z^2}$ band, as compared with 1T-TiS_2. This shift could be due to a lowering of the S 3s orbital energy by the Coulomb interaction with Sn. The energy gap between the top of the S 3s band and the bottom of the valence band is about 4.1 eV, which is smaller than for 1T-TiS_2 (about 6.80 eV), but it is close to that for hypothetical SnS.

The valence band ranges from -7.40 to $+1.28$ eV, with a width of about 8.7 eV, which is much larger than that of 1T-TiS_2 (where it is about 5.0 eV). The partial band structure of the SnS part is very similar to that of the SnS with hypothetical structure, but with a shift up of about 1.0 eV. The lower part of the valence band consists mainly of Sn 5s and

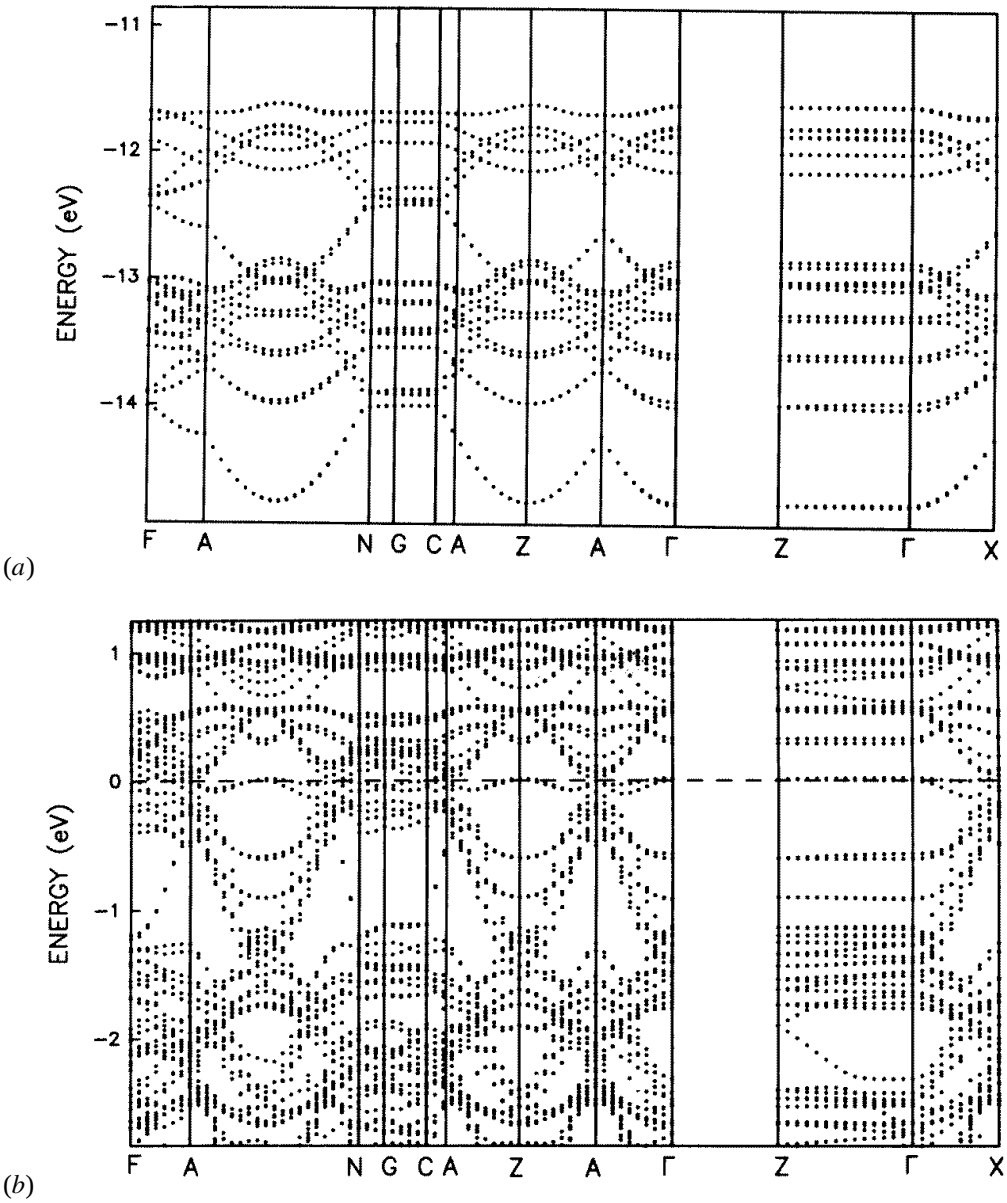

Figure 7. The dispersion of (*a*) the S 3s bands and (*b*) the bands near the Fermi level for $(SnS)_{1.20}TiS_2$.

S 3p of the SnS subsystem, and a small contribution of S 3p of the TiS_2 subsystem. The latter contribution is direct evidence for a covalent interlayer interaction between Sn 5s and S(TiS_2) 3p orbitals.

The energy bands near the Fermi level (figure 7(b)) are mainly composed of Ti 3d, S 3p orbitals of the SnS and TiS_2 subsystems, and Sn 5s states. We found that the Ti 3d states near the Fermi level consist of mainly Ti $3d_{z^2}$ orbitals. The hypothetical SnS compound is a semiconductor. However, in the calculated band structure of $(SnS)_{1.20}TiS_2$

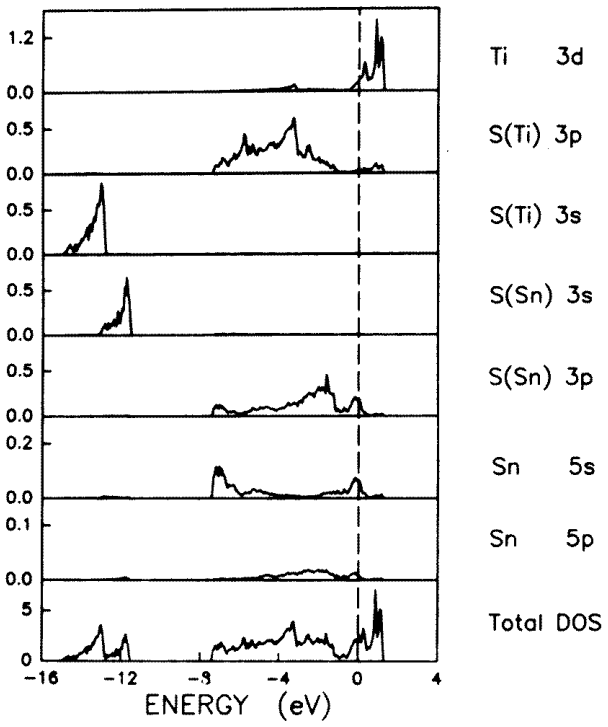

Figure 8. The total and partial DOSs of $(SnS)_{1.20}TiS_2$; S atoms in the SnS and TiS_2 subsystems are indicated as S(Sn) and S(Ti), respectively.

there are unoccupied 3p states of S atoms in the SnS subsystem, and also unoccupied Sn 5s states, which indicates charge transfer from the SnS to the TiS_2 layers. There is about 0.2–0.3 hole/SnS in the unoccupied Sn 5s and S 3p states of the SnS layers, which correponds to the about 0.2 e/Ti in the Ti 3d band. It is concluded that there is a transfer of about 0.2 e/Ti from the SnS layers to the TiS_2 layers.

The dispersion of the energy bands at the Fermi level shows a strong anisotropy (figure 7(b)). The bands near the Fermi level show a strong dispersion (about 1 eV) for directions with a $\boldsymbol{k}$ component perpendicular to $\boldsymbol{c}^*$. This dispersion is caused by strong covalent intralayer interactions in the subsystems, and is also found in the band structures of the components. At about the Fermi level one observes several bands with a dispersion of about 0.005–0.05 eV in the direction parallel to $\boldsymbol{c}^*$ (Γ–C and Γ–Z). These are primarily the bands with mainly Ti 3d and Sn 5s characters.

The bands at Γ at energies of −1.07 and −1.12 eV correspond to the Ti $3d_{z^2}$ states of the 10 Ti atoms in the primitive unit cell of $(SnS)_{1.20}TiS_2$. The width of about 1.0 eV of the Ti $3d_{z^2}$ band is about the same as in 1T-TiS_2. In $(SnS)_{1.20}TiS_2$ the bottom of Ti $3d_{z^2}$ band is 0.5 eV below the Fermi level, while for 1T-TiS_2 the bottom of Ti $3d_{z^2}$ is just at the Fermi level. This indicates a certain occupation of the Ti $3d_{z^2}$ band in the misfit layer compound, due to the transfer of electrons from the SnS to the TiS_2 subsystem. From the DOS near the Fermi level, which is mainly due to the Ti $3d_{z^2}$ band, we estimate a charge transfer of 0.2 e/Ti.

5. XPS and UPS experiments

XPS measurements of the misfit layer compound $(SnS)_{1.20}TiS_2$ have been reported by Ohno for the valence band [7] and by Ettema and Haas for the core levels [8]. However, the measurements of the valence band by Ohno have a low resolution and the S 3s band was affected by the presence of Mg K$\alpha_{3,4}$ satellites of the Sn 4d core electrons (binding energies of 24.8 and 25.7 eV) [7].

The misfit layer compound $(SnS)_{1.20}TiS_2$ was synthesized and crystals were grown by vapour transport as described before [4]. Crystals obtained were approximately squares with rounded sides, with dimensions of about 2–10 mm. We carried out XPS measurements in a small-spot ESCA machine from Vacuum Generators (VG). A spot size of 300–600 μm was used. The radiation source was an Al anode using the Kα line with a photon energy of 1486.6 eV. The sample surface was cleaned by stripping with Scotch tape in the preparation chamber at a base pressure of 10^{-9} Torr. The sample with a fresh surface was transported to the main chamber (base pressure, 10^{-10} Torr). The cleaned surface showed hardly any contamination by O and C. We also performed UPS measurements with photons of energy 21.2 eV from an He lamp.

The XPS core levels correspond quite well to those reported by Ettema and Haas [8].

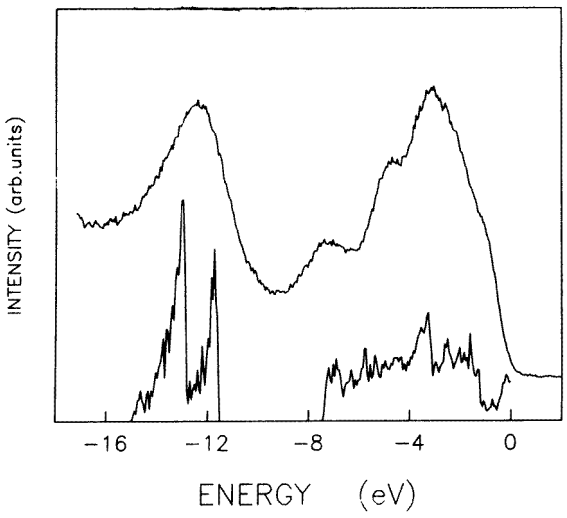

Figure 9. XPS of the valence band of $(SnS)_{1.20}TiS_2$ (top), compared with the calculated spectrum of $(SnS)_{1.20}TiS_2$ (bottom).

XPS of the valence band of the misfit layer compound $(SnS)_{1.20}TiS_2$ is shown in figure 9. A calculated spectrum deduced from the band structure is included for comparison. The calculated spectrum is obtained from the partial DOSs by multiplying by the appropriate cross section for photoemission [23]. The S 3s band is quite wide; the maximum is situated at about −12.6 eV which agrees quite well with the peaks of the calculated spectrum. This peak could not be seen in the spectra reported by Ohno due to the effect of the Mg K$\alpha_{3,4}$ satellites of Sn 4d core electrons. The valence band peak situated at about −7.5 eV corresponds to Sn 5s orbitals hybridized with S 3p (SnS part) and mixed with some S 3p states from the TiS_2 part. There is a narrow peak just below the Fermi level which corresponds mainly to Ti $3d_{z^2}$ states. Considering the resolution of the measurments (about

1.5 eV for this case) the calculated bands are in general agreement with the experimental data.

UPS of the valence band of $(SnS)_{1.20}TiS_2$ (figure 10) corresponds quite well to the results of XPS, but the resolution is much better. The first sharp peak below the Fermi level is again the Ti $3d_{z^2}$ band.

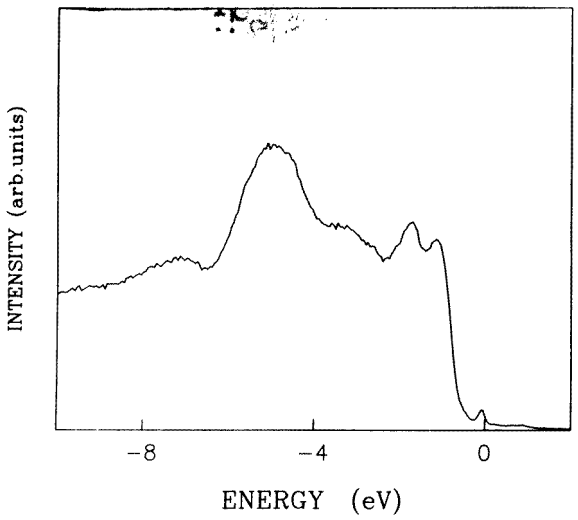

Figure 10. UPS (photon energy 21.2 eV) of the valence band of $(SnS)_{1.20}TiS_2$ (after subtracting the background).

6. Conclusions

Using a self-consistent LSW method, the electronic structure of the layer compound $(SnS)_{1.20}TiS_2$ was calculated. The results were compared with the electronic structures of the components SnS and TiS_2. From these studies we find that the band structure of the misfit compound $(SnS)_{1.20}S_2$ can be regarded approximately as a superposition of the bands of the two components. There is a small transfer of about 0.2 e/Ti from the SnS to the TiS_2 subsystem. The dispersion of some of the energy bands for a direction $\boldsymbol{k} \parallel \boldsymbol{c}^*$ shows that there is a considerable covalent interaction between the two subsystems. Using the bond valence method we find that the interlayer interactions in $(SnS)_{1.20}TiS_2$ are much stronger than in α- and β-SnS. The stability of the misfit layer compound $(SnS)_{1.20}TiS_2$ is mainly due to covalent bonding between Sn atoms and S atoms of the TiS_2 subsystem, as in the case of $(SnS)_{1.17}NbS_2$ [11]. The contribution of electrostatic interactions, as a result of charge transfer, is much smaller. The calculated electronic structure is in good agreement with experimental XPS and UPS results.

References

[1] Wiegers G A and Meerschaut A 1992 *Incommensurate Sandwiched Layered Compounds (Materials Science Forum 100 & 101)* ed A Meerschaut (Trans Tech.)

[2] Wiegers G A and Meerschaut A 1992 *J. Alloys Compounds* **178** 351

[3] van Smaalen S 1992 *Incommensurate Sandwiched Layered Compounds (Materials Science Forum 100 & 101)* ed A Meerschaut (Trans. Tech.)
[4] Wiegers G A *Prog. Solid State Chem.* at press
[5] Wiegers G A, Meetsma A, de Boer J L, van Smaalen S and Haange R J 1991 *J. Phys.: Condens. Matter* **3** 2603
[6] Wiegers G A and Haange R J 1991 *Eur. J. Solid State Inorg. Chem.* **28** 1071
[7] Ohno Y 1991 *Phys. Rev.* B **44** 1281
[8] Ettema A R H F and Haas C 1993 *J. Phys.: Condens. Matter* **5** 3817
[9] Hangyo M, Nishio T, Nakashima S, Ohno Y, Tesrashima T and Kojima N 1993 *Japan. J. Appl. Phys. Suppl.* **32–33** 581
[10] Hangyo M, Nakashima S, Hamado Y, Nishio T and Ohno Y 1993 *Phys. Rev.* B **48** 11 291
[11] Fang C M, Ettema A R H F, Wiegers G A, Haas C, van Leuken H and de Groot R A 1995 *Phys. Rev.* B **52** 2336
[12] Brown I D and Altermatt D 1985 *Acta Crystallogr.* B **41** 244
[13] Brese N E and O'Keefe M 1991 *Acta Crystallogr.* B **47** 192
[14] Ettema A R H F, de Groot R A, Haas C and Turner T S 1992 *Phys. Rev.* B **46** 7363
[15] van Leuken H, Lodder A, Czyzyk M T, Springelkamp F and de Groot R A 1990 *Phys. Rev.* B **41** 5613
[16] Williams A R, Kübler J and Gelatt C D Jr 1979 *Phys. Rev.* B **19** 6094
[17] Hedin L and Lundqvist B I 1971 *J. Phys. C: Solid State Phys.* **4** 2064
[18] Anderson O K and Jepsen O 1984 *Phys. Rev. Lett.* **53** 2571
[19] Dijkstra J, van Bruggen C F and Haas C 1989 *J. Phys.: Condens. Matter* **1** 4297
[20] Mattheiss L F 1973 *Phys. Rev.* B **8** 3719
[21] Doni E and Girlanda R 1984 *Electronic Structure and Electronic Transitions in Layered Materials* ed V Grasso (Dordrecht: Kluwer)
[22] Chianelli R R, Scanlon J C and Thomas A H 1975 *Mater. Res. Bull.* **10** 1379
[23] Yeh J J and Lindau I 1985 *At. Data Nucl. Data Tables* **32** 1